

Loading Localization by Small-Diameter Optical Fiber Sensors

Liu Rongmei^{1*}, Zhu Lujia¹, Lu Jiyun², Liang Dakai¹

1. College of Aerospace Engineering, Nanjing University of Aeronautics and Astronautics, Nanjing 210016, P. R. China;

2. College of Civil Aviation, Nanjing University of Aeronautics and Astronautics, Nanjing 210016, P. R. China

(Received 14 January 2017; revised 27 June 2017; accepted 6 August 2017)

Abstract: Structural health monitoring (SHM) in service has attracted increasing attention for years. Load localization on a structure is studied hereby. Two algorithms, i. e., support vector machine (SVM) method and back propagation neural network (BPNN) algorithm, are proposed to identify the loading positions individually. The feasibility of the suggested methods is evaluated through an experimental program on a carbon fiber reinforced plastic laminate. The experimental tests involve in application of four optical fiber-based sensors for strain measurement at discrete points. The sensors are specially designed fiber Bragg grating (FBG) in small diameter. The small-diameter FBG sensors are arrayed in 2-D on the laminate surface. The testing results indicate that the loading position could be detected by the proposed method. Using SVM method, the 2-D FBG sensors can approximate the loading location with maximum error less than 14 mm. However, the maximum localization error could be limited to about 1 mm by applying the BPNN algorithm. It is mainly because the convergence conditions (mean square error) can be set in advance, while SVM cannot.

Key words: small-diameter optical fiber sensor; structural health monitoring; loading localization; back propagation neural network; support vector machine

CLC number: TP212

Document code: A

Article ID:1005-1120(2018)02-0275-07

0 Introduction

In many industrial structures applied in aerospace and renewable energy (wind turbines), longer service life and lower costs are among major concerns^[1]. Replacing critical parts and high stress members by composite materials is a solution. Because of their higher specific strength and stiffness, composite structures are widely used^[2-4]. However, the damage mechanism of composite materials is much more complex compared with traditional isotropic metal materials. Furthermore, the mechanical properties of composite materials can be rapidly degraded when internal damage occurs^[4]. For composite structures, like those for aircraft, low velocity impacts can result in structural failure^[5-6]. Therefore, structural health monitoring (SHM) of structures needs to be performed in order to detect load, es-

pecially dynamic load^[7-8].

Among the developed technologies, optical fiber sensors have attracted considerable attention because they are lightweight, and immune to electromagnetism. Furthermore, they are flexible with sufficient strength and can be embedded into composite laminates^[9-10]. Fiber optic sensors have played a major role in smart structure applications. Because of their characters of low-cost and wavelength-encoded linear response to the measured physical parameter, fiber Bragg grating (FBG) sensors have been extensively utilized in SHM^[11-13].

FBG sensors have been utilized in impact localization. Shrestha^[5] studied localizing impact points on composite wing by analyzing signal acquired by FBG sensors. They trained data from 121 points. The maximum localization error was 35 mm. After they improved the algorithm, the

*Corresponding author, E-mail address: romme@nuaa.edu.cn.

How to cite this article: Liu Rongmei, Zhu Lujia, Lu Jiyun, et al. Loading localization by small-diameter optical fiber sensors[J]. Trans. Nanjing Univ. Aero. Astro., 2018,35(2):275-281.

<http://dx.doi.org/10.16356/j.1005-1120.2018.02.275>

maximum error was decreased to 28 mm^[6]. Chan et al.^[14] studied the bird strike in a composite UAV wing using FBG sensors. The average error was 33.6 mm for the strike location estimate. Zhu^[15] studied impact localization algorithm on an aluminum alloy structure by using a four-FBG sensing network. The maximum impact ordinate localization error was 9 mm. Small-diameter FBG sensors are preferred since they affect less on mechanical performance of host structures^[16-18].

In this paper, load localization based on small-diameter FBG sensors is proposed. Two algorithms for load localization are discussed hereby. Feasibility of the proposed approach is evaluated through an experiment involving application of a 2-D FBG sensor array. An FBG interrogator is used to measure strain on the plate. The detected strain data are trained by the two different algorithm methods. The testing results are compared.

1 Methodology

Two different algorithms are proposed to recognize the load position on a structure.

1.1 Sensing principle

Small-diameter fiber Bragg grating (SDFBG) sensors are applied to structural strain monitoring here. The core diameter of the above-mentioned fiber sensor is 7 μm , and the cladding is 80 μm .

A schematic of FBG sensor is presented in Fig. 1. As a kind of reflective sensor, FBG perceives the change of parameters through the movement of resonant wavelength. When a broadband light transmits through the grating,

the wavelength λ_B that satisfies the condition of Eq. (1) will be reflected

$$\lambda_B = 2n_{\text{eff}}\Lambda \quad (1)$$

where n_{eff} is the effective refractive index of FBG and Λ the period of grating.

With the assumption of no temperature change, the Bragg wavelength will change with axial strain on optical fiber. The relative change in FBG wavelength $\Delta\lambda$ with axial strain ϵ_z can be expressed as^[19]

$$\frac{\Delta\lambda_B}{\lambda_B} = S_\epsilon \epsilon_z \quad (2)$$

where S_ϵ is the relative strain sensitivity of a FBG sensor. For a common FBG, whose core is made of silicon oxide, the sensitivity S_ϵ is 0.784.

1.2 Support vector machine theory

Support vector machine (SVM) is a learning method based on statistical learning theory^[20-21]. It is successfully used in prediction, pattern detection and classification.

Given a set of training data, i. e. $\{(x_1, y_1), \dots, (x_n, y_n)\}$, $x_i \in X \subseteq \mathbf{R}^n$, $y_i \in Y \subseteq \mathbf{R}$, x_i is the input data and y_i the corresponding target value. The SVM tries to estimate target values by using the following linear equation^[22]

$$f(x) = \mathbf{w}^T \mathbf{x}_i + b \quad (3)$$

where $f(x)$ is the output, \mathbf{w} the n -dimensional vector and b a scalar.

By using a Vapnik ϵ -insensitive loss function, the optimal linear regression function can be obtained as a solution to the following optimization^[23]

$$\min \left[\frac{1}{2} \mathbf{w}^2 + C \sum_{i=1}^n (\xi_i^+ + \xi_i^-) \right] \quad (4)$$

The following condition is to be satisfied

$$\begin{cases} \epsilon + \xi_i^- \leq y_i - \mathbf{w}^T \mathbf{x}_i - b \leq \epsilon + \xi_i^+ & i = 1, \dots, n \\ \xi_i^- \geq 0, \xi_i^+ \geq 0 & i = 1, \dots, n \end{cases} \quad (5)$$

The calculation can be simplified by converting the problem into the equivalent Lagrangian dual problem^[22].

With a kernel function as $K(\mathbf{x}_i, \mathbf{x}) = \varphi(\mathbf{x}_i) \cdot \varphi(\mathbf{x})$, the estimation of the SVM is obtained

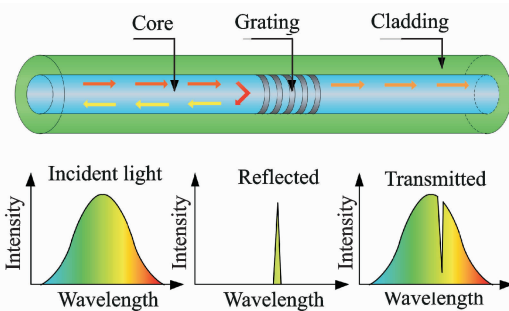


Fig. 1 Schematic of FBG sensing

by Eq. (6)^[24]

$$f(\mathbf{x}) = \sum_{i=1}^l (a_i - a_i^*) K(\mathbf{x}_i, \mathbf{x}) + b \quad (6)$$

where a_i , a_i^* are the Lagrange multipliers.

1.3 Back propagation neural network algorithm

BP neural network has been one of the most widely used algorithms^[25]. The network contains at least three parts: One input layer, at least one hidden layer, and one output layer. The input layer receives and distributes the input pattern. The hidden layers capture the nonlinearities of the input/output relationship. The output layer produces the output pattern. The structure of the BP neural network is shown in Fig. 2.

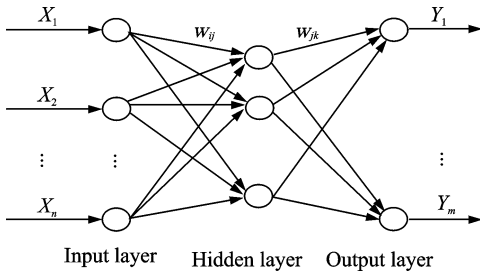


Fig. 2 Structure of a BP neural network

In the network, every neuron in each layer receives total input from all of the neurons in the previous layer. The relation is shown^[24]

$$p_j = \sum_{i=0}^N w_{ij} x_i + b_j \quad (7)$$

where p_j is the total input and N the number of inputs to the unit j in next layers, w_{ij} the weight coefficient, b_j threshold value, and x_i the input from unit i in the preceding layer. Then the output O_j of unit j can be calculated by processing the input through a transfer function $f(x)$ as

$$O_j = f(p_j) \quad (8)$$

Hereby the function $f(x)$ is optional and selected as

$$f(x) = \frac{1}{1 + e^{-x}} \quad (9)$$

Based on BP neural network, the data are trained by a series of input/output pattern sets, which are repeatedly presented to the network. The error between the actual data and the predicted output is used to adjust the weight. The net-

work will gradually learn the relationship between the input and the output by adjusting the weights. When the error of the test set reaches its minimum, network training completes and the weights are fixed.

1.4 Load orientation

As a load is applied to a structure, the structure deforms. SDFBG sensors on the structure will detect the deformation. Load positions are changed during the test. Sensors will record the deformation changes. Therefore, historical database is built on the basis of recorded data. Afterwards, the data will be trained by algorithm till the loading discriminate is accomplished. Consequently, the orientation is achieved. As the structure is loaded, the captured data is denoted as real-time data. After the real-time data are input, the load would be located.

The discriminate procedure is sketched in Fig. 3.

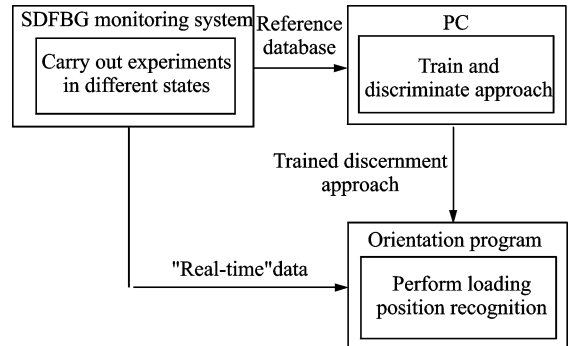


Fig. 3 Process of load orientation

In training and discrimination procedures, SVM and BP algorithms are applied, respectively. Therefore, two orientation programs are set. The feasibility of the proposed methods is evaluated experimentally.

2 Experiment

Optical fiber-based sensors were applied to monitoring a designed carbon fiber reinforced plastic (CFRP) laminate. The size of the laminate is 600 mm × 600 mm × 2.16 mm. The laminate is clamped on edges by specially de-

signed clamps with a width of 30 mm.

Four small-diameter FBG sensors were glued on the back of the laminate, as shown in Fig. 4. The working length of the used Bragg is 10 mm. A local coordinate is set as shown in Fig. 4. The positions and the original central wavelengths of the sensors are listed in Table 1.

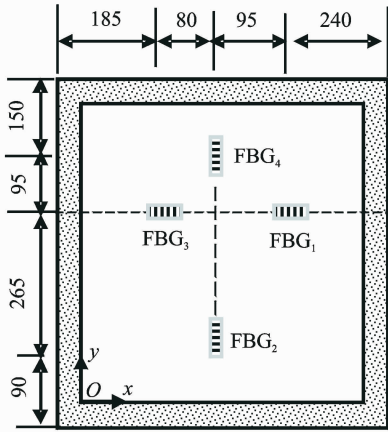


Fig. 4 Schematic of sensors on the monitored laminate

Table 1 Details of FBG sensors

Sensor	Central wavelength / nm	Location / mm
FBG ₁	1 527. 111	(330,325)
FBG ₂	1 527. 970	(235,60)
FBG ₃	1 528. 435	(155,325)
FBG ₄	1 526. 953	(235,420)

A FBG demodulator SI425 from Micron Optics Inc was used to capture the central wavelength of the sensor array. The experimental set-up is shown in Fig. 5. The work area of the plate is 540 mm × 540 mm, which is divided into 12 parts on each side.

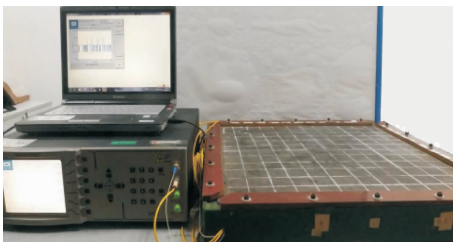


Fig. 5 Experimental setup

As the temperature is constant, a weight of 3 kg is slowly put on the surface of the plate. The weight stands at different grids. The wavelengths of four sensors are recorded every time. Together 65 signals are acquired. Among the detected data, 58 are taken as reference data at random. The left data, i. e. , seven data are chosen as tested ones.

3 Results and Discussions

The reference database is trained by using SVM and BP neural network separately. The seven load localizations are predicted. The results are shown in Fig. 6.

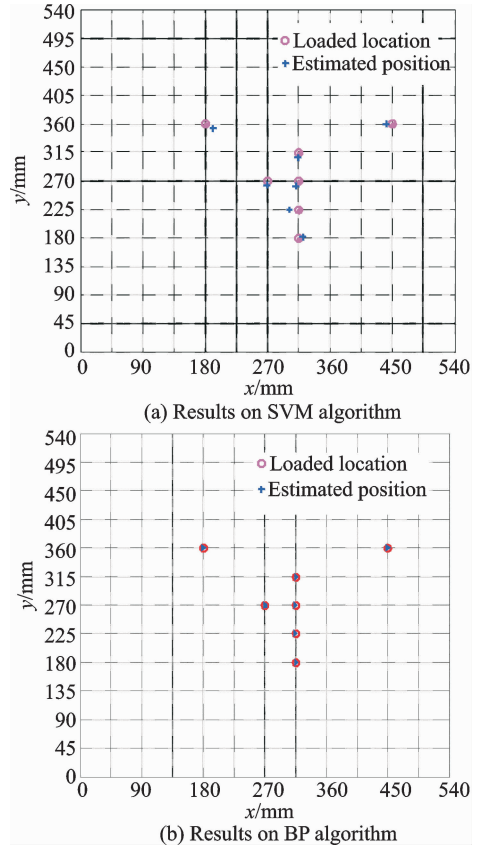


Fig. 6 Estimated load positions

The details of the tested load positions are illustrated in Table 2. According to SVM results, the maximum location error are 13. 669 mm and 9. 248 mm in x and y directions, respectively. However, the maximum error is 1. 124 mm in x direction, and 0. 015 mm in y direction based on the BP algorithm.

Table 2 Tested load positions

No.	Loaded position / mm		SVM estimated position / mm		BP estimated position / mm	
	<i>x</i> -coordinate	<i>y</i> -coordinate	<i>x</i> -coordinate	<i>y</i> -coordinate	<i>x</i> -coordinate	<i>y</i> -coordinate
1	180	360	191.163	352.813	180.003	360.003
2	270	270	269.293	263.080	270.056	270.000
3	315	180	321.393	181.039	315.898	179.991
4	315	225	301.331	223.827	313.876	225.015
5	315	270	311.231	262.036	314.496	269.998
6	315	315	313.165	305.752	315.676	314.997
7	450	360	440.755	359.296	449.998	360.000

Obviously, the predictive position is closer to the actual location according to the results by the BP algorithm. The reason may lie in the difference between the two training methods. When the data are trained by means of the BP procedure, a neural network which has marvelous approximation would be built. The network is trained to calculate the weights which minimize the mean square error (MSE) between network prediction and training data. The weights are updated until it converges to a certain value.

The training performance by BP is shown in Fig. 7, where the best training performances are 0.040 0307 and 0.001 989 8 at 539 and 897 epochs, respectively. In our study, the MSE of the training data is set to 0.002. It can be observed that the MSE gradient descends until it approaches the set value. The training process takes about 4 s for 897 iterations.

4 Conclusions

Loading position detection methods based on discrete strain have been proposed. The strain measurements are implemented by four small-diameter FBG sensors arranged in a 2-D array. Development of the methods involves use of a reference database by two different training techniques, namely SVM and BP neural network. The methods are evaluated experimentally on a 540 mm × 540 mm CFRP laminate.

Experimental results indicate that the 2-D small-diameter FBG sensors can estimate the planar loading location even with less data. The maximum error is less than 14 mm by using SVM

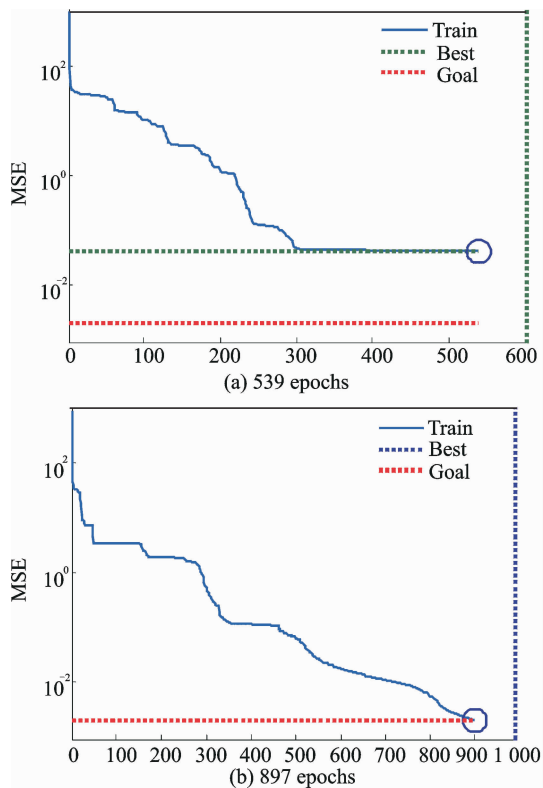


Fig. 7 Training performance by BP procedure

method and could be limited to about 1 mm by the BP neural network algorithm. The testing error difference between the two methods is due to the difference in the training.

If the loading amplitudes are changed besides the loading positions, the predictive method is similar. However, more complicated algorithms are needed to predict both the loading positions and the loading amplitudes.

Acknowledgements

This work was supported by the National Natural Science Foundation of China (Nos. 11402112, 51405223).

References:

- [1] LICARI J, UGALDE-LOO C E, EKANAYAKE J B, et al. Comparison of the performance and stability of two torsional vibration dampers for variable-speed wind turbines[J]. *Wind Energy*, 2014, 18(9):1545-1559.
- [2] VANNIAMPARAMBIL P A, CARMÍ R, KHAN F, et al. An active-passive acoustics approach for bond-line condition monitoring in aerospace skin stiffener panels[J]. *Aerospace Science and Technology*, 2015, 43:289-300.
- [3] MOGHADDAM M K, BREEDE A, CHALOUPKA A, et al. Design, fabrication and embedding of microscale interdigital sensors for real-time cure monitoring during composite manufacturing[J]. *Sensors and Actuators A: Physical*, 2016, 243: 123-133.
- [4] NORRIS C J, WHITE J A P, MCCOMBE G, et al. Autonomous stimulus triggered self-healing in smart structural composites[J]. *Smart Materials and Structures*, 2012, 21: 094027.
- [5] SHRESTHA P, KIM J H, PARK Y, et al. Impact localization on composite wing using 1D array FBG sensor and RMS/correlation based reference database algorithm[J]. *Composite Structures*, 2015, 125:159-169.
- [6] SHRESTHA P, KIM J H, PARK Y, et al. Impact localization on composite structure using FBG sensors and novel impact localization technique based on error outliers[J]. *Composite Structures*, 2016, 142: 263-271.
- [7] WANG Z, WANG J, SUI Q, et al. Deformation reconstruction of a smart Geogrid embedded with fiber Bragg grating sensors[J]. *Measurement Science and Technology*, 2015, 26(12): 125202.
- [8] BAO T, BABANAJAD S K, TAYLOR T, et al. Generalized method and monitoring technique for shear-strain-based bridge weigh-in-motion[J]. *Journal of Bridge Engineering*, 2015, 21(1):1-13.
- [9] MINAKUCHI S, TAKEDA N. Recent advancement in optical fiber sensing for aerospace composite structures[J]. *Photonic Sensors*, 2013, 3(4):345-354.
- [10] LUYCKX G, VOET E, LAMMENS N, et al. Strain measurements of composite laminates with embedded fiber Bragg gratings: criticism and opportunities for research[J]. *Sensors*, 2011, 11(1): 384-408.
- [11] LAI M, FRIEDRICH K, BOTSIS J, et al. Evaluation of residual strains in epoxy with different nano/micro-fillers using embedded fiber Bragg grating sensor[J]. *Composites Science and Technology*, 2010, 70: 2168-2175.
- [12] RAZALI N F, BAKAR M H A, TAMCHEK N, et al. Fiber Bragg grating for pressure monitoring of full composite lightweight epoxy sleeve strengthening system for submarine pipeline[J]. *Journal of Natural Gas Science and Engineering*, 2015, 26:135-141.
- [13] ZHU Nannan, ZHANG Jun. Multi-wavelength fiber sensor for measuring surface roughness based on laser scattering[J]. *Infrared & Laser Engineering*, 2016, 45(5) : 225-231. (in Chinese)
- [14] CHAN Y P, JANG B W, KIM J H, et al. Bird strike event monitoring in a composite UAV wing using high speed optical fiber sensing system [J]. *Composite Science and Technology*, 2012, 72 (4) : 498-505.
- [15] ZHU X. Aluminum alloy material structure impact localization by using FBG sensors[J]. *Photonic Sensor*, 2014, 4(4): 344-348.
- [16] LIU R M, LIANG D K. Natural frequency detection of smart composite structure by small diameter fiber Bragg grating[J]. *Journal of Vibration and Control*, 2015, 21: 2896-2902.
- [17] TAKEDA S I, OGASAWARA T, YOKOZEKI T. Damage monitoring of polymer-lined carbon fibre-reinforced plastic using small-diameter fibre Bragg grating sensors[J]. *Journal of Reinforced Plastics and Composites*, 2015, 34(6) : 454-462.
- [18] LIU R M, LIANG D K, ASUNDI A. Small diameter fiber Bragg gratings and applications[J]. *Measurement*, 2013, 46(9):3440-3448.
- [19] PANOPOULOU A, LOUTAS T, ROULIAS D, et al. Dynamic fiber Bragg gratings based health monitoring system of composite aerospace structures[J]. *Acta Astronautica*, 2011, 69: 445-457.
- [20] SPILLMAN W B, SIRKIS J S, GARDINER P T. Smart materials and structures: what are they? [J]. *Smart Materials and Structures*, 1996, 5(3):245-254.
- [21] NAJAFI G, GHOBADIAN B, MOOSAVIAN A, et al. SVM and ANFIS for prediction of performance and exhaust emissions of a SI engine with gasoline - ethanol blended fuels[J]. *Applied Thermal Engineering*, 2016, 95: 186-203.
- [22] WIDODO A, YANG B S. Support vector machine in machine condition monitoring and fault diagnosis[J]. *Mechanical Systems and Signal Processing*, 2007, 21: 2560-2574.
- [23] BURGESS C J C. A tutorial on support vector machines for pattern recognition[J]. *Data Mining and Knowledge Discovery*, 1998, 2(2):955-974.

- [24] XU Y, YOU T, DU C. An integrated micromechanical model and BP neural network for predicting elastic modulus of 3-D multi-phase and multi-layer braided composite[J]. *Composite Structures*, 2015, 122: 308-315.
- [25] WU B, HAN S, XIAO J, et al. Error compensation based on BP neural network for airborne laser ranging [J]. *Optik*, 2016, 127: 4083-4088.

Dr. **Liu Rongmei** received her B. S. and M. S. degrees in Materials Science and Engineering from Nanjing University of Aeronautics & Astronautics (NUAA) in 1997 and 2000, respectively. In 2011, she obtained her Ph. D. in Testing. She chose smart materials as her area of specialization. From 2002, she has been an associate professor of

the College of Aerospace Engineering, NUAA. Her research interest focuses on optical fiber based sensors.

Mr. **Zhu Lujia** is a post graduate student in NUAA. His research interest focuses on optical fiber smart composite materials.

Dr. **Lu Jiyun** is a lecturer of College of Civil Aviation at NUAA. She graduated from the University of Jilin with a bachelor degree of science in photoelectronic technique in 2002. She received her Ph. D. degree in Engineering from NUAA. Her research interest mainly focuses on FBG sensor and its engineering applications.

Prof. **Liang Dakai** received his B. S. and Ph. D. degrees in Testing from NUAA. He won the third prize for national invention in 1998. Now his research interest focuses mainly on intelligent materials and structures.

(Production Editor: Zhang Tong)

